

Rock typing in the Upper Devonian-Lower Mississippian Woodford Shale Formation, Oklahoma, USA

Ishank Gupta¹, Chandra Rai¹, Carl Sondergeld¹, and Deepak Devegowda¹

Abstract

Most U.S. shale plays are spatially extensive with regions of different thermal maturity and varying production prospects. With increasing understanding of the heterogeneity, microstructure, and anisotropy of shales, efforts are now directed to identifying the sweet spots and optimum completion zones in any shale play. Rock typing is a step in this direction. We have developed an integrated workflow for rock typing using laboratory-petrophysical measurements on core samples and well logs. A total of seven wells with core data were considered for rock typing in the Woodford Shale. The integrated workflow has been applied in the Woodford Shale in a series of steps. In the first step, unsupervised clustering algorithms such as *K*-means and self-organizing maps were used to define the rock types. Rock type 1 is generally characterized by high porosity and total organic carbon (TOC). Rock type 2 had intermediate values of porosity and TOC and thus, moderate source potential and storage. Rock type 3 had the highest carbonate content, poor storage, and source rock potential. In the next step, a classification algorithm, support vector machines (SVM), was used to extend the rock types from the cores to the logs. A logging suite with gamma ray, resistivity, neutron porosity, and density logs was used for extending the rock types. These logs were used because they are commonly available and adequate to differentiate different rock types. The rock types were populated in the uncored sections of the seven cored wells and additionally in 12 wells (taken from Drilling Info) using a trained SVM model. Additional wells were taken to have sufficient data for production correlation. In the final step, a rock-type ratio (RTR) was defined based on the fraction of rock type 1 over the gross thickness. RTR was found to positively correlate with normalized oil equivalent production.

Introduction

The number of successful wells has increased steadily from 65% in 1974 to 90% in 2010, where a successful well is defined as a well completed as an oil or gas production well (Williams, 2012). This improvement is attributed to improved data quality, quantity, interpretation, and superior drilling technology. Rock typing is one of the reservoir characterization techniques leading to integration of data from multiple sources and thereby improving interpretation. The term “rock types,” as defined in this study, refers to different types of rock categorized based on similarity in petrophysical properties.

In conventional reservoirs, most commonly used rock-typing techniques, such as R35 (Kolodzie, 1980; Gunter et al., 2014), RP35 (Aguilera, 2002), RQI, and FZI (Amaefule et al., 1993; Corbett and Potter, 2004), require core-derived permeability-porosity data. The rock typing can also be carried out with well log-derived porosity and permeability values. Although well logs do not provide direct estimates of permeability, several

correlations have been developed for permeability estimation (Timur, 1968; Coates and Dumanoir, 1974; Thomeer, 1983). The application of such rock-typing techniques was largely restricted to sandstones and carbonates that are characterized by a large range of porosity and permeability values.

Conventional techniques are not adequate in unconventional reservoirs because of the lack of dynamic range of porosity and permeability. Second, permeability measurements on shale samples in the laboratory are difficult to make and may not be accurate. In addition, other key variables, such as hydrocarbon source potential and brittleness, are not considered in conventional rock-typing methods because conventional reservoirs generally do not have in situ hydrocarbon generation or do not require hydraulic fractures to produce economic quantities of oil/gas.

Kale et al. (2010) carry out rock typing for the Barnett Shale and include several petrophysical parameters, such as total organic carbon (TOC), mineralogy,

¹The University of Oklahoma, Mewbourne School of Petroleum and Geological Engineering, Norman, Oklahoma, USA. E-mail: ishank@ou.edu; crai@ou.edu; csongergeld@ou.edu; deepak.devegowda@ou.edu.

Manuscript received by the Editor 31 January 2017; revised manuscript received 9 November 2017; published ahead of production 21 November 2017; published online 10 January 2018. This paper appears in *Interpretation*, Vol. 6, No. 1 (February 2018); p. SC55–SC66, 14 FIGS., 1 TABLE. <http://dx.doi.org/10.1190/INT-2017-0015.1>. © 2018 Society of Exploration Geophysicists and American Association of Petroleum Geologists. All rights reserved.

helium porosity, and mercury injection capillary pressure (MICP). [Sondhi \(2011\)](#) uses a similar approach for the Eagle Ford Shale, whereas [Gupta \(2012\)](#) and [Gupta et al. \(2013\)](#) perform rock typing for the Woodford Shale Formation. Other recent approaches to rock typing in shales are discussed by [Aranibar et al. \(2013\)](#), [Li et al. \(2015\)](#), and [Gupta et al. \(2017\)](#).

This study focuses on the Woodford Shale Formation. The paper is organized as follows: (1) a description of the core-derived measurements that form the inputs to the rock typing, (2) a description of the use of clustering algorithms such as self-organizing maps (SOMs) ([Kohonen and Honkela, 2007](#)) and *K*-means clustering ([Macqueen, 1967](#)) to derive meaningful rock types from core data, and (3) an extension of the rock typing procedure to a regional level via a supervised classification technique called the support vector machines (SVM) ([Cortes and Vapnik, 1995](#)).

Laboratory measurements used for rock typing

The rock typing was done using laboratory measurements of porosity (via helium), mineralogy, TOC, and source-rock analysis (SRA) data. The helium porosity was measured using the technique developed by [Karastathis \(2007\)](#). In Karastathis's method, the bulk volume is measured using a mercury-immersion technique. Boyle's law is used to measure the grain volume in a porosimeter. Finally, the helium porosity is calculated from bulk and grain volumes.

Mineralogical composition was determined using Fourier transform infrared spectroscopy (FTIR) ([Sondergeld and Rai, 1993](#); [Ballard, 2007](#)). The absorbance spectrum is inverted to give composition in terms of weight percent of 16 different minerals, such as quartz, calcite, dolomite, illite, smectite, kaolinite, chlorite, pyrite, orthoclase, oligoclase, mixed clays, albite, anhydrite, siderite, apatite, and aragonite. FTIR was used because it is cheaper

and gives a better quantification of clays compared with XRD ([Sondergeld and Rai, 1993](#)).

TOC measurements were done using the LECO TOC apparatus ([Law, 1999](#)). SRA data were acquired using a Rock-Eval instrument (pyrolysis flame-ionization detection technique). The S1 and S2 peaks from SRA are indicative of source-rock potential. S1 represents the movable fraction of the TOC, whereas S2 represents the immovable fraction. A description of the method is given by [Law \(1999\)](#).

Description of the study area

The robustness of the rock typing is directly tied to the extent of the coring program. Ideally, cores should be acquired across a range of depths to provide adequate representation of the stratigraphic and spatial variability in the formation. For the Woodford Shale, several wells with core data were available that were also geographically distributed over the play. The workflow used for rock typing is given in Figure 1.

The Woodford Shale is an Upper Devonian-Lower Mississippian shale located in the Anadarko, Arkoma, Ardmore, and Marietta Basins of Oklahoma and Texas. It has produced more than 87 MMbbl oil, and 4.6 Tcf gas so far (Drilling Info, May 2017). In the prolific parts of the Woodford Shale play (South-Central Oklahoma Oil Province [SCOOP]), the thickness of the Woodford Formation varies between 45.7 and 121.9 m (150 and 400 ft) ([CLR, 2010](#)).

The Woodford Shale in Oklahoma is an organic-rich, dark-gray mudstone. It was formed along a west-to-southwest facing, arid, passive continental margin in an epeiric sea during a time when persistent oceanic upwelling coincided with marine transgression ([Comer, 2008](#)). Initially, there was a single basin called the Oklahoma Basin ([Johnson, 1988](#)), which later gave rise to the four basins, namely, the Anadarko, Ardmore, Arkoma, and Marietta Basins. The four basins separated after a post-Woodford, Pennsylvanian orogenic episode ([Gupta, 2012](#); [Gupta et al., 2013](#)). The Silurian age Hunton Limestone is a widespread unconformity, and it defines the base of the Woodford Shale formation in most of the places. During the late Devonian, North America moved north and thus, placing the southern midcontinent near 15°–20° south latitude, as indicated by paleogeographic reconstruction. This caused frequent upwelling and temperate climate in the Oklahoma Basin, which facilitated high biologic production and the resultant TOC enrichment of the Woodford Shale.

The common lithologies found in the Woodford Formation are argillaceous shale, siliceous shale, siliceous-dolomitic shale, black chert, siliceous mudstone, and dolomitic mudstone (H. Galvis, personal communication, 2017). The argillaceous shale, siliceous shale, and siliceous-dolomitic shale facies are rich in clays compared with black chert and siliceous mudstone facies. The latter are rich in quartz. Quartz in Woodford have different sources and distributions. Quartz can be detrital and biogenic (chert). Biogenic quartz represents

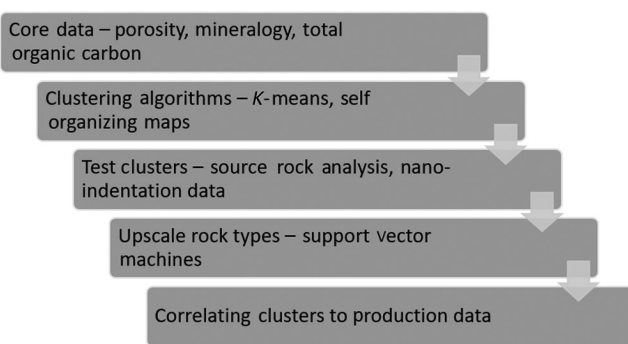


Figure 1. The workflow used in this study for rock typing in the Woodford Shale. The first step is extensive data collection in the laboratory on cored wells. The second step involves clustering the data to establish different rock types. Next, clusters are tested using ancillary core data to check their robustness. Then, the rock types are extended to logs. Finally, rock-type logs are analyzed with production data to ascertain the key rock type controlling the production.

siliceous radiolaria. The source of quartz in argillaceous shale, siliceous shale, and siliceous-dolomitic shale facies is primarily detrital, whereas in chert and siliceous mudstone facies, it is primarily biogenic.

Comer (2005) reports TOC and vitrinite reflectance data for the Woodford Shale. The data show that the Anadarko Basin has a high TOC and it lies in the oil maturity window. Thus, the Anadarko Basin is likely to have high oil production in the Woodford Shale. The SCOOP and

Sooner Trend Anadarko Basin Canadian and Kingfisher Counties, the most prolific Woodford Shale regions, lie in the Anadarko Basin.

The wells containing core and well-log data that were used for rock typing are shown in Figure 2. Most of these wells are in the Anadarko Basin (shown as red bubbles). Core data were available for 411 depths in the seven cored wells. Triple combo logs (gamma ray, neutron, density, and resistivity) were available

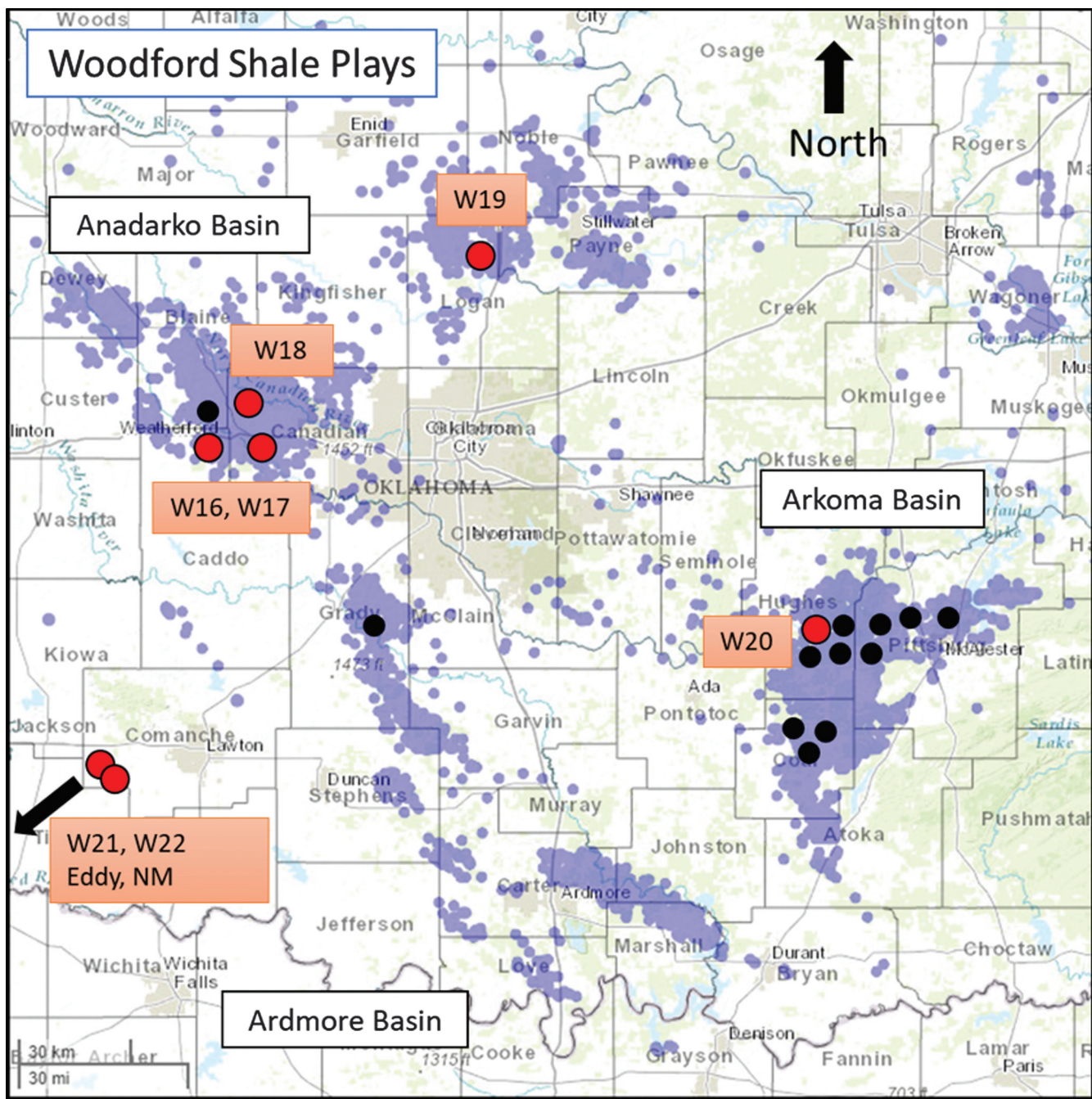


Figure 2. Wells with core and triple combo log data used for rock typing within the study area. Seven wells had core data (shown as red bubbles), most of which were in the Anadarko Basin. Core data were available for 411 depths. An additional 12 wells (shown as black bubbles) had triple combo logs, but no core data. Rock-type logs were populated in all 19 wells for comparison with production data. The Woodford Shale top varies from approximately 1828 m (6000 ft) in the southeast (Arkoma Basin) to more than 3657 m (12,000 ft) in the northwest (Anadarko Basin), thereby indicating a large vertical and areal coverage.

in all the seven wells, and they were used for extending the rock types from core to log level. In addition, 12 wells (shown as black bubbles) without core data but with triple combo logs were incorporated into

the study for production correlation. The logs from these wells were used to generate rock-type logs for comparison with the production data from these wells.

Rock-typing methodology

The key petrophysical parameters used for rock typing are porosity, TOC, and mineralogical compositions, namely, quartz, carbonate, and clay content (Kale, 2009; Kale et al., 2010; Gupta et al., 2017). These data were selected as pores, minerals, and organic matter form the basic constituents of any shale rock, and they strongly influence major petrophysical properties of interest, which in turn determine shale deliverability. These five parameters were also used because they were consistently available for all 411 core depths. The other data, namely, SRA, ultrasonic, and MICP were sporadically available only for a fraction of the total depth intervals. In addition, Kale et al. (2010) show that these five parameters explain the maximum variance in the data.

Figure 3 shows the histograms of the different variables used for rock typing. The histograms show that all the variables have almost normal distribution. The distribution for carbonate content is not shown because generally all the samples have low carbonate content except for a few samples that have a very high carbonate content. Within the few samples containing high carbonates, some samples have predominantly calcite, whereas others have predominantly dolomite. The TOC distribution is slightly skewed to the left, whereas the clay distribution is slightly skewed to the right. The advantage of using clustering techniques such as *K*-means and SOM is that they can handle multidimensional data sets with different distributions (James et al., 2013).

The bivariate analysis is shown through several crossplots in Figure 4. The first three plots show the variation of porosity with TOC, clays, and quartz, respectively. It is evident that porosity shows a weak positive correlation with all three parameters, suggesting that all three parameters contribute to porosity. TOC contributes to organic porosity, whereas clays and quartz contribute to inorganic porosity. TOC shows a weak negative correlation with clays for this data set. There is no clear correlation with quartz and carbonates. The logs were not available in all the cored wells, and, thus, the Upper, Middle, and Lower Woodford could not be identified for all the cored depths. However, based on limited data, it is apparent that the Lower Woodford has the highest clay fraction and lowest quartz fraction among the different zones. The Middle Woodford has clay-rich and quartz-rich facies.

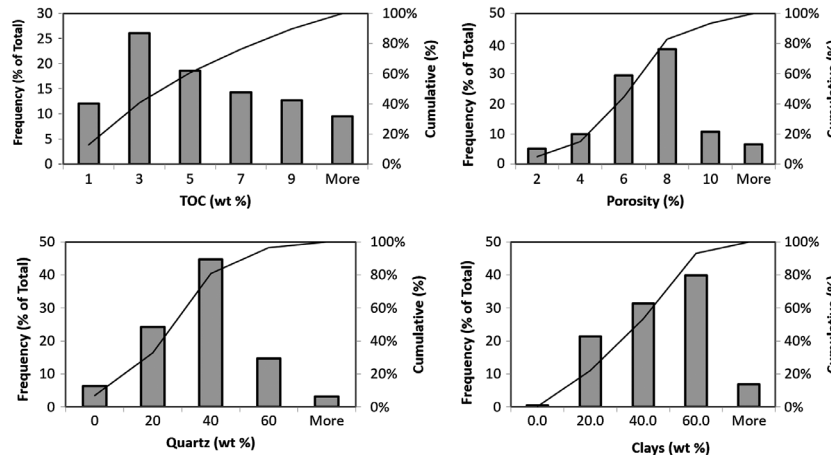


Figure 3. Histograms for different variables used for rock typing show that all the variables have almost normal distribution. The TOC distribution is slightly skewed to the left, whereas clay distribution is slightly skewed to the right. The advantage of using clustering techniques such as *K*-means and SOM is that they can handle multidimensional data sets with different distributions.

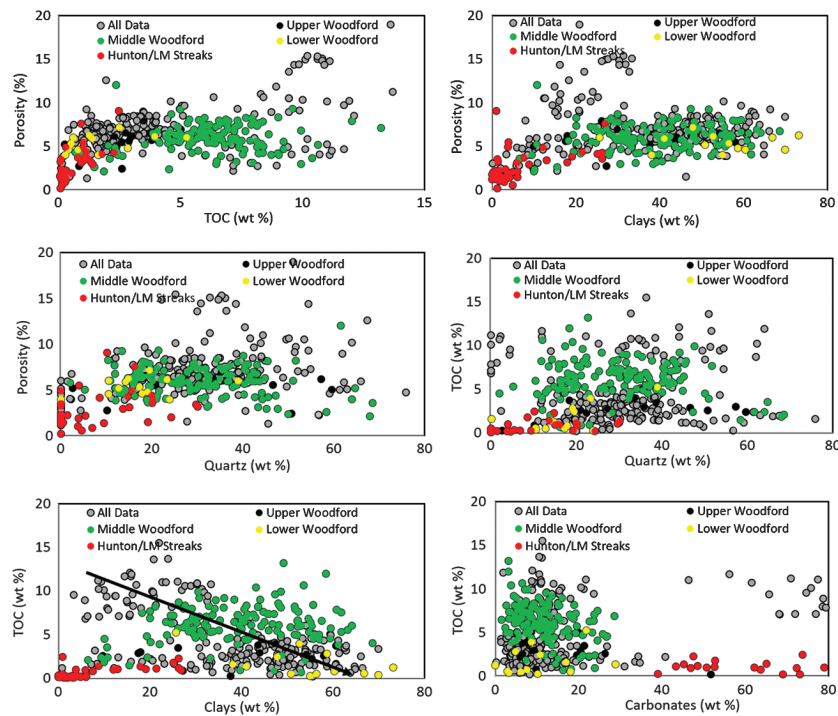


Figure 4. The bivariate analysis is shown through several crossplots. It is evident that porosity shows a weak positive correlation with all three parameters, suggesting that all three parameters contribute to porosity. TOC contributes to organic porosity, whereas clays and quartz contribute to inorganic porosity. TOC shows a weak negative correlation with clays for this data set. There is no clear correlation with quartz and carbonates. The logs were not available in all the cored wells, and, thus, the Upper, Middle, and Lower Woodford could not be identified for all the cored depths. However, based on limited data, it is apparent that the Lower Woodford has the highest clay fraction and lowest quartz fraction among the different zones. The Middle Woodford has clay-rich and quartz-rich facies.

correlation with clays for this data set. There is no clear correlation with quartz and carbonates. The logs were not available in all the cored wells, and thus, the Upper, Middle, and Lower Woodford could not be identified for all cored depths. However, based on limited data, it is apparent that the Lower Woodford has the highest clay fraction and lowest quartz fraction among the different zones. The Middle Woodford has clay-rich and quartz-rich facies. The different crossplots show that there are nonlinear relationships between different petrophysical parameters and properties, such as porosity, are dependent on several parameters. Thus, multivariate analysis, which can consider these different relationships, is expected to be more suitable for rock-typing analysis.

Because input data had high dimensionality, principal component analysis (PCA) (Hotelling, 1933) was used to reduce the dimensionality of the data set. The idea behind PCA is to identify directions in multidimensional space that contain most of the variations observed in the data. Principal components are linear combination of different input parameters (TOC, porosity, quartz, clay, and carbonate content in this study). In general, the first few principal components explain most of the variance in the data. Figure 5a shows the plot of principal components versus variance in the data. In this data set (Woodford), the first three principal components explain 90% of the variance in the data. Thus, instead of using five variables (such as TOC, porosity, quartz, clay, and carbonate content) for clustering, it is sufficient if we use the first three principal components.

Clustering algorithms, such as *K*-means and SOM (Chon and Park, 2008) can now be used in the reduced dimensional space to define rock types. The data variability can be exploited to deter-

mine the optimum number of clusters. The optimum number of clusters is chosen to be three in this study because of the analysis presented in Figure 5b, which plots intracluster (red curve) and intercluster variances (green curve) as a function of the number of clusters. Intracluster variance refers to the average variance within a cluster. Intercluster variance refers to the variance between the clusters. The point at which the curves or plots become asymptotic defines the optimum number of clusters. In this study, the optimum number of clusters was found to be three. Finally, *K*-means was used to create three clusters, and the results are shown in Figure 5c.

SOM is another popular clustering algorithm that provides a 2D representation of a more complex, multi-dimensional data set (Pang, 2003). The three clusters identified from SOM are shown in Figure 6a. The characteristics of the three clusters are shown in the rose diagram (or pie diagram) in Figure 6b. The rose diagram shows that rock type 1 (RT1) has the highest porosity and highest TOC. The diagram also shows that rock type 3 (RT3) is associated with high carbonates, low porosity, and low TOC. Comparison of SOM and *K*-means cluster-

Table 1. Mean and standard deviations for different petrophysical properties for different rock type groups have been listed. The numbers enclosed in parenthesis represent number of core measurements categorized as that rock type by *K*-means/SOM.

Woodford	TOC (wt%)	Porosity (vol%)		Carbonate (wt%)		Clays (wt%)		Quartz (wt%)		S1 (mg/g)		
	Mean	Std.	Mean	Std.	Mean	Std.	Mean	Std.	Mean	Std.	Mean	Std.
RT 1 (120)	6.6	3.3	7.7	3.6	14.2	6.8	24.6	8.9	46.5	11.8	3.6	3.1
RT 2 (231)	3.8	2.3	6.4	1.4	9.5	6.9	48.3	9.4	25.8	8.9	2.4	2.3
RT 3 (060)	2.6	3.8	3.1	1.7	76.9	16.5	7.5	7.9	6.6	9.8	1.1	0.8

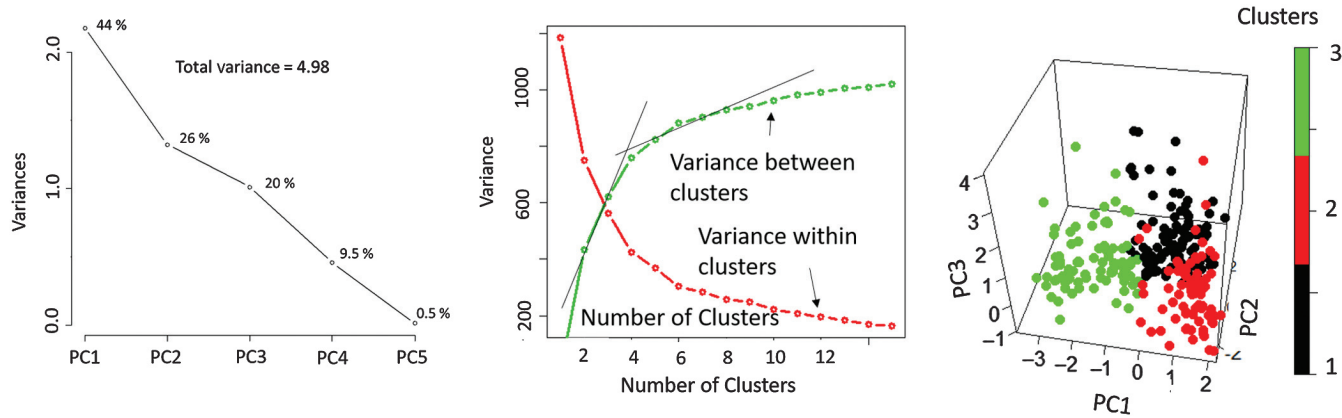


Figure 5. The *K*-means clustering schematic. (a) PCA. PCA is used to reduce the dimensionality of the clustering problem. The key principal components are used for rock typing, which explains the maximum variance in the data and (b) determination of an optimum number of clusters requires analysis of the intracluster variance (red curve) and intercluster variance (green curve). Intracluster variance refers to the average variance within a cluster. Intercluster variance refers to the variance between the clusters. The point at which the curves or plots become asymptotic defines the optimum number of clusters (in this case three to four rock types). (c) Three clusters obtained using *K*-means plotted in 3D. Each axis is one principal component.

ing provided very similar results. Table 1 shows the characteristics of different rock types obtained from *K*-means and SOM clustering techniques for the Woodford.

Finally, rock types obtained from petrophysical measurements on plugs are extended to the logs using SVM-based (Steinwart and Christmann, 2008) classification. SVM is a supervised learning model that constructs classifiers based on well logs that are trained to recognize the previously described core-derived rock types. The idea behind the construction of a classifier is to identify a plane that separates distinct clusters (or rock types). Such a plane is called a hyperplane. Examples of hyperplanes are shown in Figure 7 for linear and non-linear classifications between the blue- and red-colored points.

For the rock-typing application, the SVM model was trained using the depth intervals for which core and log data are available. A calibration data set was prepared that included core-derived rock types, gamma ray, neutron, density, and resistivity values from depths at which log and core data were available. A large part of the calibration data set was used to train the model, and then a prediction

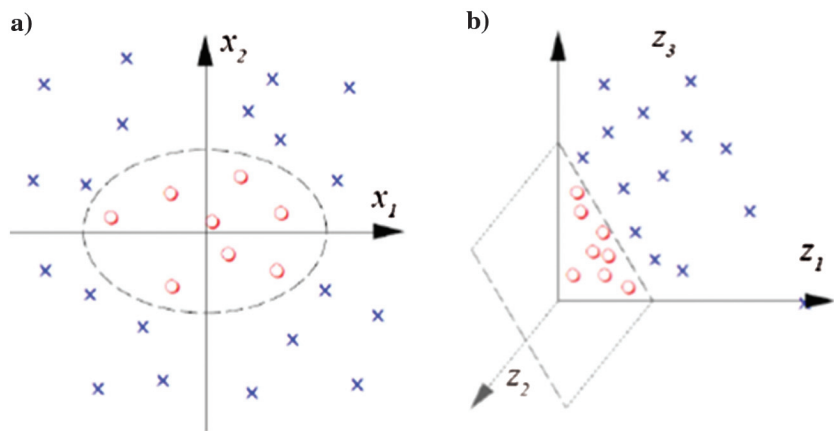


Figure 7. Examples of hyperplane in SVM. The separation between different clusters is termed a hyperplane, and its geometry can be linear, polynomial, or radial. (a) An example of radial hyperplane and (b) an example of a linear hyperplane.

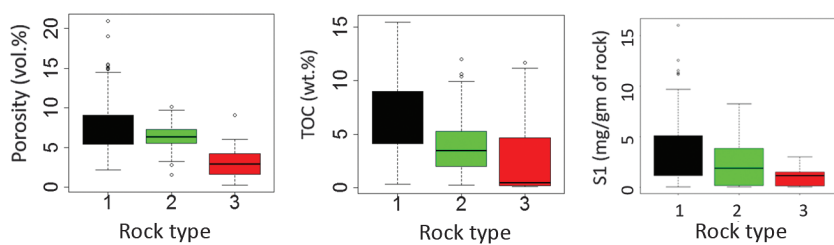


Figure 8. Parameters governing storage and source potential in the Woodford Shale. Clearly, rock type 1 has the highest porosity, TOC, and S1 values. Porosity is a direct indicator of storage potential. A high amount of TOC and large S1 values generally suggest a higher source-rock potential. Thus, rock type 1 has the highest storage and source potential.

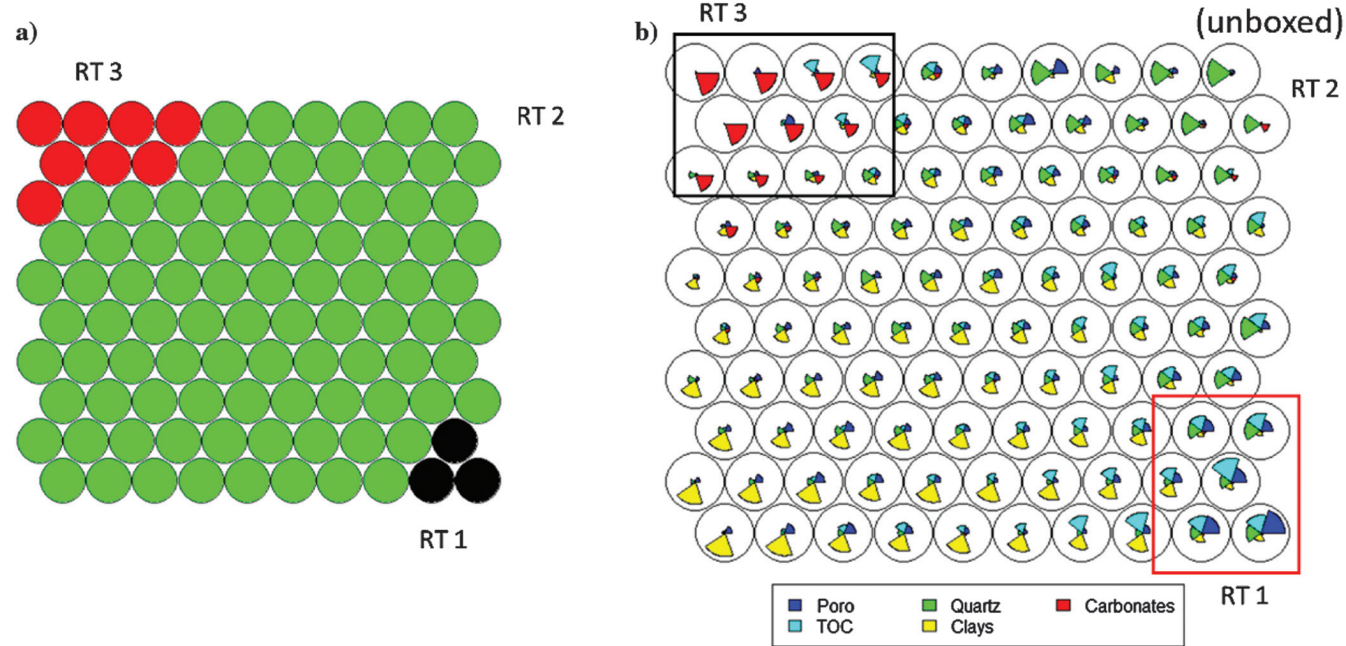


Figure 6. (a) Clusters created on an SOM map and (b) Rose diagram (or pie diagram) from SOM. The rose diagram shows the characteristics of different rock types/clusters. RT1 is of high porosity and high TOC. RT3 is carbonate rich. RT2 is of a lower TOC, lower porosity, and is clay-rich. The relative fraction of different rock types shown on the rose diagram/SOM map is not representative of actual fraction of different rock types in the core data. The three clusters obtained from SOM are similar to those obtained from *K*-means (more than 80% of the core samples predict the same rock type).

was made on a small portion of the data set. The efficiency or accuracy of the classifier was gauged by the predictions of the rock type from the SVM classifier against those obtained from the core data. The radial SVM model gave the best results, and, therefore, it was used for prediction. The radial model is more flexible than the linear model. Any data that can be separated by a linear hyperplane can also be separated by a radial hyperplane. There are more complicated models that require data transformation, but they are not required in this exercise. Readers are advised to try several models and use the one that gives the best prediction of the predicted rock types versus the core-derived rock types. The trained model was then used to predict rock types for the remaining depths in the cored wells and in wells in which core data were unavailable. The distribution of the rock types along the wellbore was then correlated with the production data to identify the key rock type controlling the production.

Results and discussion

Core-derived rock typing

The different rock types were analyzed with respect to their petrophysical response. Porosity is a direct indicator of storage potential, TOC is the total organic content, and S1 signifies the amount of movable hydrocarbons in the core. High values of TOC and S1 peaks generally indicate higher source rock potential, assuming a given level of thermal maturity.

The parameters governing storage and source potential for different rock types in the Woodford Shale are shown in Figure 8. Rock type 1 has the highest porosity, TOC, and S1 values. The average mineral content for the different mineral groups in the three rock types is shown in Figure 9. Rock type 1 has a high quartz content. Rock type 2 has the highest clay percentage. Thus, different rock types have different mineralogies. Coupled with high TOC and porosity, rock type 1 is expected to have a large contribution to production.

Stratigraphic analysis was not done as a part of this study. Based on the convention (H. Galvis, personal communication, 2017), the major lithofacies encountered by the samples used in this study are argillaceous shale, siliceous shale, siliceous-dolomitic shale, siliceous mudstone, and dolomitic mudstone. Rock type 1 is likely rich in siliceous shale and siliceous mudstone. On the other hand, rock type 2 is likely rich in argillaceous shale, whereas rock type 3 is rich in dolomitic mudstone. Rock type 3 mainly comprises of the cal-

careous streaks and a few samples cored in Hunton limestone.

MICP data were also available for 112 core samples. The capillary pressure curves were evaluated for each of the three rock types to see if the different rock types were different with respect to the capillary pressure curves. Incremental and cumulative Hg intrusion plots,

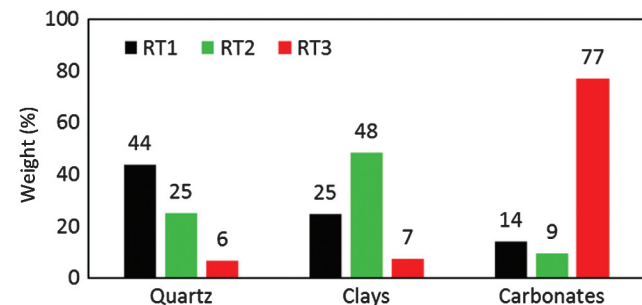


Figure 9. Average mineral content for different rock types in the Woodford Shale. Rock type 1 has a high quartz content. Rock type 2 has the highest clay percentage. Thus, different rock types have different mineralogies.

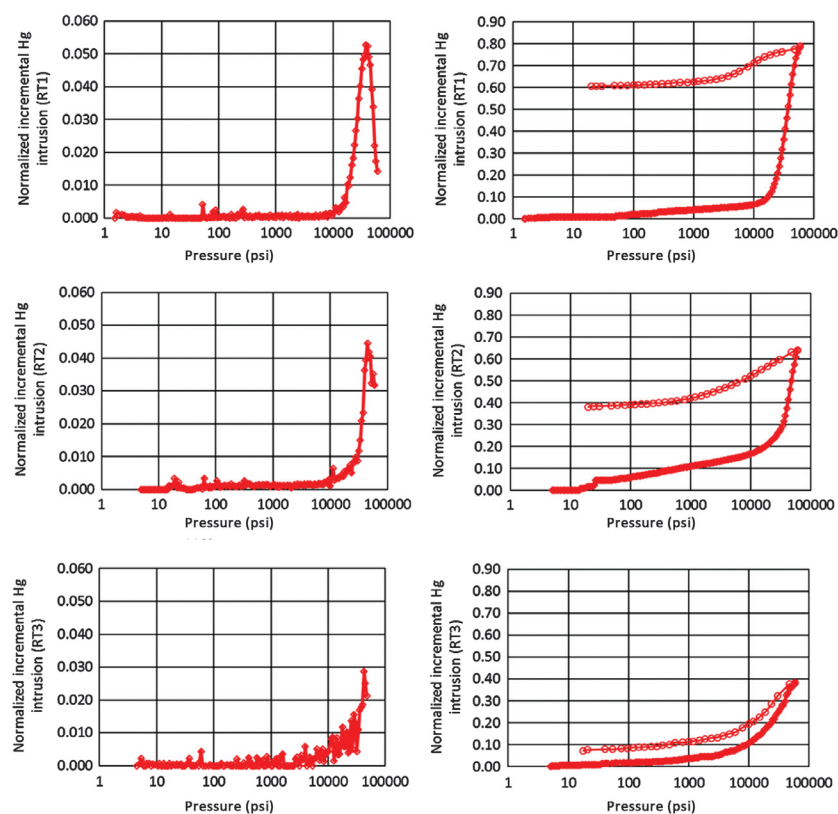


Figure 10. Normalized incremental and cumulative mercury intrusion plots for the three rock types. Rock type 1 is characterized by large hysteresis and largest dominant pore-throat radius of 6 nm. Rock type 2 is characterized by large hysteresis and a smaller dominant pore-throat size of 4 nm. Rock type 3 has a continuously increasing intrusion curve implying that the dominant pore-throat radius may be smaller than 3 nm (60,000 psia, the limit of the mercury-injection apparatus). In addition, rock type 3 has little hysteresis, which might indicate false intrusion. Thus, connectivity and expected permeability decreases as we go from the best to the worst rock type.

normalized by helium pore volume for the three rock types, are shown in Figure 10. The incremental intrusion plots show the data obtained during the intrusion cycle only, whereas cumulative intrusion plots include data points from the intrusion and extrusion cycle.

In rock type 1 samples, which had the highest storage and source rock potential, the cumulative intrusion

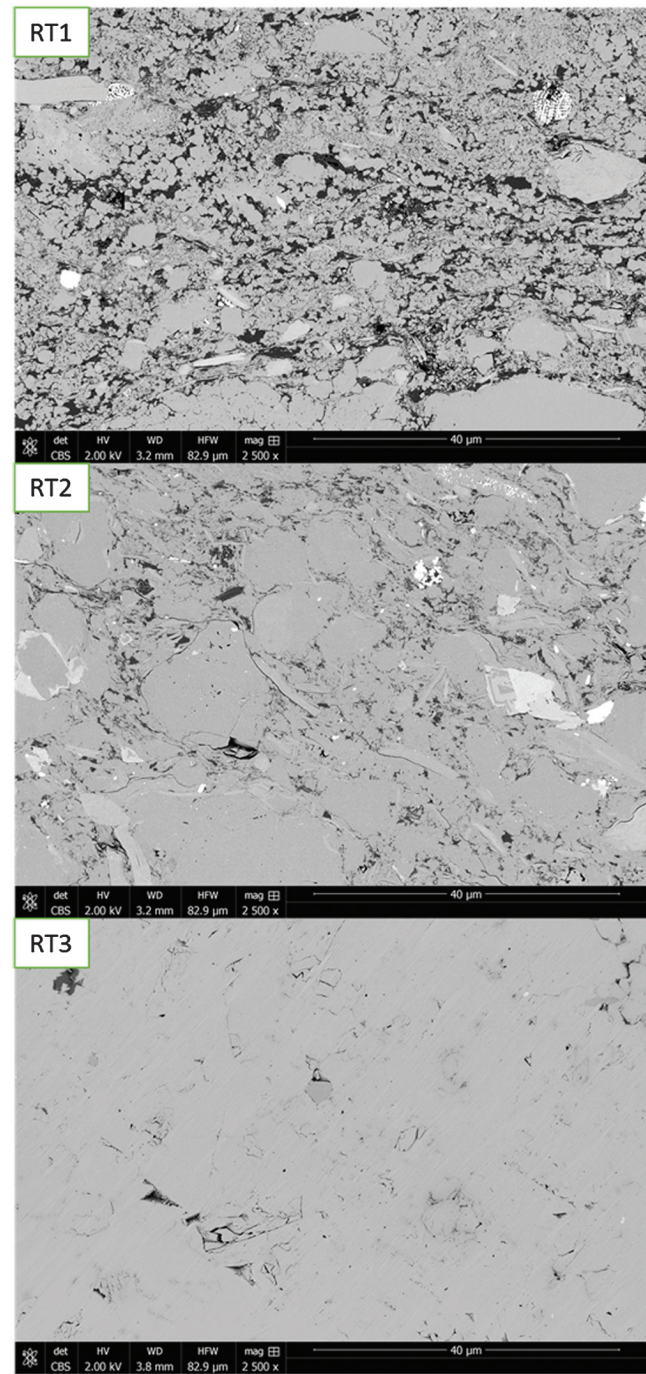


Figure 11. The SEM images for samples belonging to the three rock-type groups. The darker shades, dark gray, and black represent organic matter and pores, respectively. The lighter shades (light gray) represent different mineral groups, such as quartz, carbonate, clays, etc. It is evident that the organic matter (TOC) and porosity decrease from RT1 to RT3.

plot shows that the ratio of mercury to helium pore volume varies between 0.65 and 0.80. In rock type 2 samples, this ratio varies between 0.50 and 0.65, and it varies between 0.40 and 0.55 for rock type 3 samples. Thus, it shows the connected pore volume decreases as we go from rock type 1 to rock types 2 and 3. The interesting fact is that rock types 1 and 2 had a high range of helium porosity, but rock type 2 had lower connectivity than rock type 1. This is likely due to its clay-rich nature where clays, present at the pore lining and pore throats, reduce the connectivity.

The shape of the capillary pressure curve also clearly distinguishes the three rock types. In rock type 3, the curves for the samples increases continuously without reaching a plateau or an inflection point even at 60,000 psia. At 60,000 psia, equivalent pore size that the mercury could pass through is 3 nm. This shape is characteristic of very tight rocks in which the dominant pore size may be smaller than 3 nm. These samples are characterized by a high carbonate percentage and have a higher grain density.

The cumulative intrusion plots in rock types 1 and 2 exhibit considerable hysteresis between saturating and desaturating curves, implying that not all the Hg that enters the sample during the intrusion cycle comes out when the pressure is released during the extrusion cycle. This is an evidence that Hg is indeed intruding into the rock. However, in rock type 3, cumulative intrusion curves in rock type 3 exhibit almost overlapping saturating and desaturating curves. A lack of hysteresis between saturating and desaturating curves is a sign of false intrusion due to sample and Hg compression at high pressures.

In rock types 1 and 2 samples, the capillary pressure curve exhibits a distinct maximum before 60,000 psia. The inflection point reflects the dominant pore throat. Samples dominated by a proportionally greater number of larger pore throats should possess higher permeability. For rock type 1 samples, the average dominant pore-throat size was 6 nm, whereas for rock type 2 samples, it was 4 nm. Thus, rock type 1 samples would be expected to have the highest permeability. As discussed before, rock type 2 samples may be affected by the presence of clay.

Scanning electron microscope (SEM) images are indicative of the microstructure and should be characteristically different for different rock types. Figure 11 shows SEM images for samples belonging to the three rock type groups. The darker shades, dark gray and black, represent organic matter and pores, respectively. The lighter shades (light gray) represent different mineral groups, such as quartz, carbonate, clays, etc. It is evident that the organic matter (TOC) and porosity decrease from RT1 to RT3.

Extending core-based classification to well logs

We next extended the core-based classification to the well-log data. This is necessary because in general, not all intervals within a well are cored and additionally,

it would be necessary to determine the distribution of rock types in the uncored wells for mapping purposes.

A classification technique called SVMs was used for extending the core-based classification to the log data.

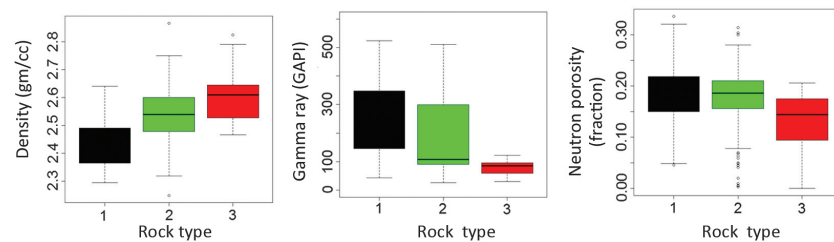


Figure 12. Gamma ray, density, and neutron-logs distribution for the three rock types in the Woodford Shale. Rock type 1 has low density, high gamma ray, and high neutron porosity consistent with high TOC and high laboratory-measured porosity. The TOC can show a high gamma-ray signature at the log due to enhanced radioactivity by the trace uranium generally associated with the organic matter. Rock type 3, on the other hand, has highest density and lowest neutron porosity consistent with high carbonates in laboratory-measured mineralogy.

This technique uses a calibration data set for training the model. The calibration data set consisted of core-derived rock-type values and log (gamma ray, neutron, density, and resistivity) values extracted for the same depth intervals. The SVM technique is an iterative technique that predicts the rock type using the log values at a particular depth and then compares the predicted rock type with the actual value derived from K-means or SOM. This process is carried out until most of the predicted rock types are the same as those derived from core data. At this point, the SVM model is said to be trained. The trained model was then used to predict rock types in uncored wells and the remaining section of the cored wells where core data were not available.

Figure 12 shows the distribution of gamma ray, neutron porosity, and den-

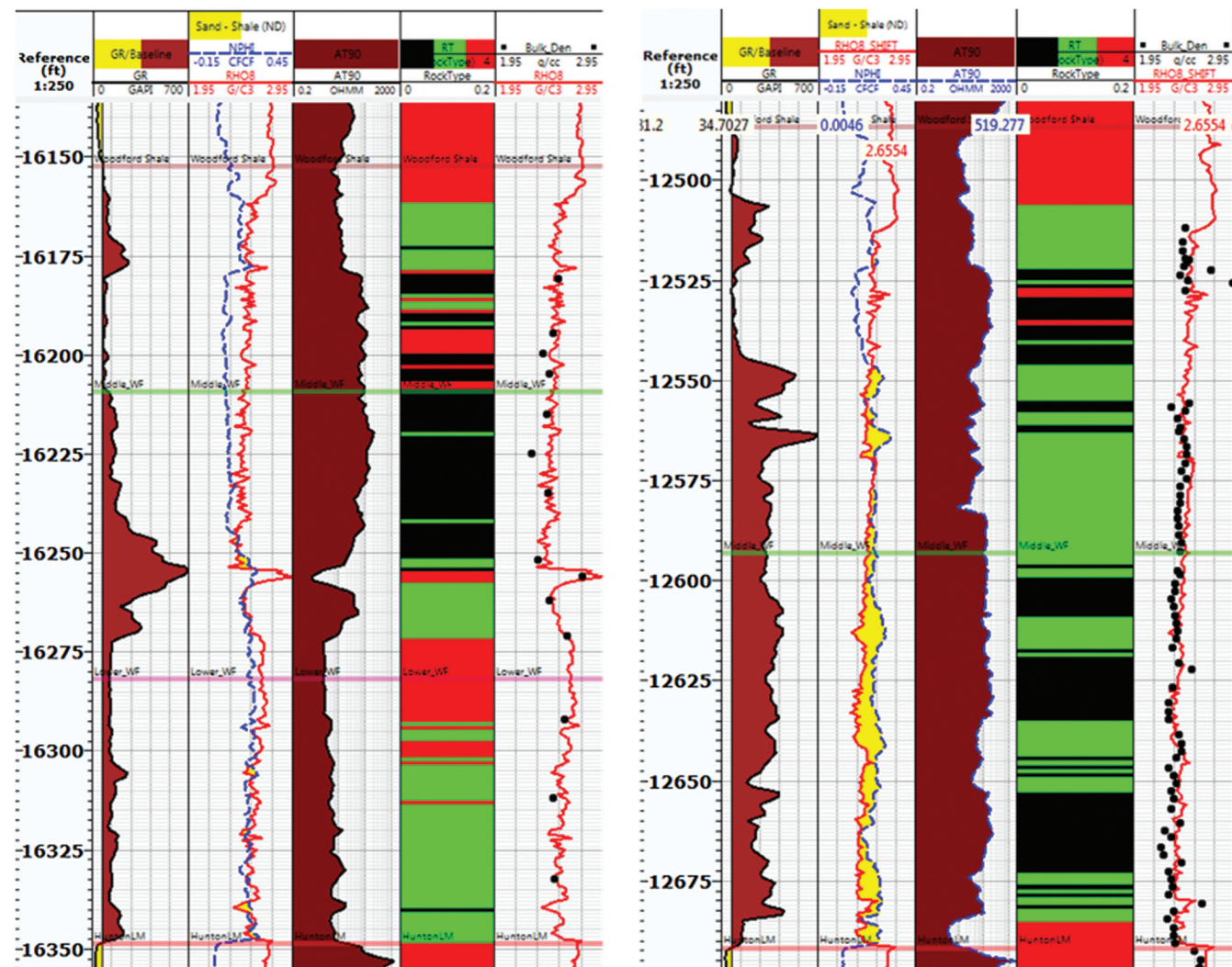


Figure 13. Rock-type logs for two sample wells (W1 on left, W3 on right) in the Woodford Shale. The sixth track shows a comparison between bulk density log and bulk density of the core samples measured in the laboratory. In track 5, black represents RT1, green represents RT2, and red represents RT3.

sity logs for different rock types. Rock type 1 has low density, high gamma ray, and high neutron porosity consistent with high TOC and high laboratory-measured porosity. TOC can show high gamma-ray signature at the log due to enhanced radioactivity by the trace uranium generally associated with the organic matter. Rock type 3, on the other hand, has the highest density and lowest neutron porosity consistent with high carbonates in laboratory-measured mineralogy. The logs were consistent with the core data, and they were found adequate for extending the rock types. Figure 13 shows the rock-type logs for two sample wells (W1 on the left, W3 on the right).

Relating rock types to production data

Rock type 1 has the highest storage and source rock potential. Thus, rock type 1 is expected to be the key driver of the production. A rock type 1 ratio (RTTR) was created by dividing the rock type 1 thickness with the gross thickness (i.e., RT1 + RT2 + RT3) for all the wells. The RTTR was then correlated with normalized 24 months cumulative production. The positive correlation between the two validates the robustness and practical utility of the rock-typing exercise carried out in this study.

The spatial locations of the wells for which rock types were extended are shown in Figure 2. The red represents wells with cores, and the black represents additional wells that did not have core data. Some of the wells were horizontal, and some were vertical. All the cores belong to the vertical sections. To make a fair comparison, the production was normalized by the lateral lengths for horizontal wells and the zone thickness for vertical wells. Figure 14 shows a comparison of RTTR with normalized production. Normalized production here refers to the first 24 months of cumulative barrel

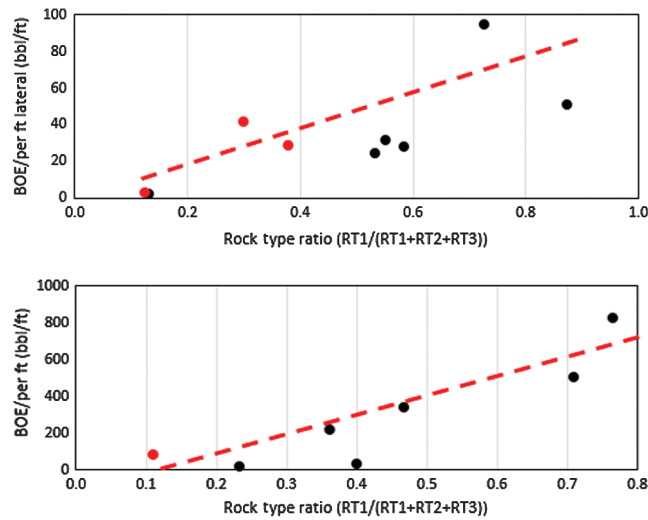


Figure 14. Normalized production correlated with the RTTR in Woodford. The red bubbles represent cored wells, and the black bubbles represent additional wells. (a) Correlation plot for horizontal wells. (b) Correlation plot for vertical wells. A positive correlation is evident on both the plots suggesting that rock type 1 is the key rock type controlling the production.

of oil equivalent normalized by the lateral length or zone thickness. A positive correlation between normalized production and RTTR is evident. The spread in the plots is likely due to different completion efficiencies and fracture treatments (data for which were not available). This is because production is a multivariable problem affected by reservoir properties such as porosity, permeability, brittleness, etc. and completion efficiencies such as fracture conductivity, landing zone, formation damage, etc.

Conclusion

The current paper presents results for rock typing in the Woodford Shale. The rock types were first derived using laboratory measurements, namely, TOC, porosity, quartz, clay, and carbonate content. Data mining algorithms, such as *K*-means, SOM, SVM, etc., are very powerful in handling a large amount of data and finding meaningful associations between different data types. The rock types can aid the reservoir or production engineer in selecting sweet spots. Rock type 1 is the best reservoir rock. It has the highest storage and source rock potential. Therefore, rock type 1 can be selectively perforated to save completion costs and maximize production from a well. On the other hand, rock type 3 is poor reservoir and may not warrant any perforation.

The core-derived rock types were extended to log data using a classification technique called SVM. Thus, rock-type logs were generated as a result in 19 wells more than 1219 m (4000 ft) interval. These logs were then used to calculate a RT1 ratio (fraction of rock type 1 over gross thickness), which showed a positive correlation with the production from the wells. Future work would include carrying out extensive stratigraphic correlation and correlating different rock type units with stratigraphic sections and regional geology to understand how source rocks and sweet spots develop.

These applications represent a fraction of the true potential of the rock typing. Some applications of the rock typing that were not carried out in this paper but can realize the true potential of rock typing are 3D reservoir modeling, identifying sweet spots in combination with seismic attributes, new well locations, improved volumetric estimates, and uncertainty and risk analysis. These applications require rock-type logs in many wells (approximately >30%) in any field. The success of an extensive coring program governs the robustness of the rock typing. The greater the reservoir that is sampled, the better the rock typing.

Acknowledgments

We would like to thank Devon, Cimarex, and Drilling Info for providing the cores and logs to carry out the study. Their generous contribution has made this study possible. We would also like to thank all the reviewers for providing valuable inputs and key insights to the study.

References

- Aguilera, R., 2002, Incorporating capillary pressure, pore throat aperture radii, height above free water table and Winland R35 values on Pickett plots: AAPG Bulletin, **86**, 605–624, doi: [10.1306/61EEDB5C-173E-11D7-8645000102C1865D](https://doi.org/10.1306/61EEDB5C-173E-11D7-8645000102C1865D).
- Amaefule, J. O., M. Altunbay, D. Tea, D. G. Kersey, and D. K. Keelan, 1993, Enhanced reservoir description: Using core and log data to identify hydraulic (flow) units and predict permeability in uncored intervals/wells: Annual Technical Conference and Exhibition, SPE, doi: [10.2118/26436-MS](https://doi.org/10.2118/26436-MS).
- Aranibar, A., M. Saneifar, and Z. Heidari, 2013, Petrophysical rock typing in organic-rich source rocks using well logs: Unconventional Resources Technology Conference, SPE/AAPG/SEG, doi: [10.1190/URTEC2013-117](https://doi.org/10.1190/URTEC2013-117).
- Ballard, B. D., 2007, Quantitative mineralogy of reservoir rocks using Fourier transform infrared spectroscopy: International Student Paper Contest, SPE, doi: [10.2118/113023-STU](https://doi.org/10.2118/113023-STU).
- Chon, T. S., and Y.S. Park, 2008, Self-organizing map, in S. E. Jorgenson and B. D. Fath, eds., Encyclopedia of ecology: Academic Press, 3203–3210.
- CLR, 2010, Anadarko Woodford: The SCOOP, <http://jhpenenergy.com/wp-content/uploads/2015/10/2.pdf>, accessed 20 January 2017.
- Coates, G. R., and J. L. Dumanoir, 1974, A new approach to improved log-derived permeability: The Log Analyst, **15**, 17–31.
- Comer, J. B., 2008, Woodford Shale in southern midcontinent, USA: Transgressive system tract marine source rocks on an arid passive continental margin with persistent oceanic upwelling: AAPG Annual Meeting, AAPG Search and Discovery, Article #90078.
- Comer, J. B., 2005, Facies distribution and hydrocarbon production potential of Woodford Shale in the southern midcontinent: Unconventional Energy Resources in the Southern Midcontinent Symposium, Oklahoma Geological Survey Circular, **110**, 51–62.
- Corbett, P. W. M., and D. K. Potter, 2004, Petrotyping: A basemap and atlas for navigating through permeability and porosity data for reservoir comparison and permeability prediction: Presented at the International Symposium, SCA.
- Cortes, C., and V. Vapnik, 1995, Support-vector networks: Machine Learning, **20**, 273–297, doi: [10.1007/BF00994018](https://doi.org/10.1007/BF00994018).
- Gunter, G. W., D. R. Spain, E. J. Viro, J. B. Thomas, G. Potter, and J. Williams, 2014, Winland pore throat prediction method: A proper retrospect: New examples from carbonates and complex systems: Presented at the 55th Annual Logging Symposium, SPWLA.
- Gupta, I., C. Rai, C. Sondergeld, and D. Devegowda, 2017, Rock typing in Wolfcamp Formation: Presented at the 58th Annual Logging Symposium, SPWLA.
- Gupta, N., 2012, Multi-scale characterization of the Woodford Shale in west-central Oklahoma from scanning electron microscope to 3D seismic: Ph.D. thesis, University of Oklahoma.
- Gupta, N., C. Rai, and C. Sondergeld, 2013, Petrophysical characterization of Woodford Shale: 54th Annual Logging Symposium, SPWLA, Extended Abstracts, 368–382.
- Hotelling, H., 1933, Analysis of a complex of statistical variables into principal components: Journal of Educational Psychology, **24**, 417–441 (498–520), doi: [10.1037/h0071325](https://doi.org/10.1037/h0071325).
- James, G., D. Witten, T. Hastie, and R. Tibshirani, 2013, An introduction to statistical learning with applications in R: Springer.
- Johnson, K. S., 1988, Geologic evolution of the Anadarko basin, in K. S. Johnson, ed., Anadarko Basin Symposium: Oklahoma Geological Survey Circular, 3–12.
- Kale, S., 2009, Petrophysical characterization of Barnett Shale play: M.S. thesis, University of Oklahoma.
- Kale, S., C. Rai, and C. Sondergeld, 2010, Rock typing in gas shales: Annual Technical Conference and Exhibition, SPE, doi: [10.2118/134539-MS](https://doi.org/10.2118/134539-MS).
- Karastathis, A., 2007, Petrophysical measurements on tight gas shale: M.S. thesis, University of Oklahoma.
- Kohonen, T., and T. Honkela, 2007, Kohonen network: Scholarpedia.
- Kolodzie, S. J., 1980, The Analysis of pore throat size and use of Waxman-Smit to determine OOIP in Spindle field, Colorado: 55th Annual Fall Technology Conference and Exhibition, SPE, doi: [10.2118/9382-MS](https://doi.org/10.2118/9382-MS).
- Law, C., 1999, Evaluating source rocks: Handbook of petroleum geology: Exploring for Oil and Gas Traps, **6**, 1–41.
- Li, H., B. Hart, M. Dawson, and E. Radjef, 2015, Characterizing the middle Bakken: Laboratory measurement and rock typing of the Middle Bakken formation: Unconventional Technology Conference, SPE, doi: [10.2118/178676-MS](https://doi.org/10.2118/178676-MS).
- MacQueen, J. B., 1967, Some Methods for classification and analysis of multivariate observations: Proceedings of the 5th Berkeley Symposium on Mathematical Statistics and Probability, University of California Press, 281–297, <https://projecteuclid.org/euclid.bsmsp/1200512992>.
- Pang, K., 2003, Self-organizing maps, <https://www.cs.hmc.edu/~kpang/mn/som.html0>, accessed 25 May 2017.
- Sondergeld, C. H., and C. S. Rai, 1993, A new concept of quantitative core characterization: The Leading Edge, **12**, 774–779, doi: [10.1190/1.1436968](https://doi.org/10.1190/1.1436968).
- Sondhi, N., 2011, Petrophysical characterization of the Eagle Ford shale: M.S. thesis, University of Oklahoma.
- Steinwart, I., and A. Christmann, 2008, Support vector machines: Information science and statistics: Springer.
- Thomeer, J. H., 1983, Air permeability as a function of three pore network parameters: Journal of Petroleum Technology, **35**, 809–814, doi: [10.2118/10922-PA](https://doi.org/10.2118/10922-PA).

- Timur, A., 1968, An investigation of permeability, porosity, and residual water saturation relationship for sandstone reservoirs: *The Log Analyst*, **9**, 8–18.
- Williams, J. L., 2012, Energy economist: Wells and politics, <http://www.energyeconomist.com/a6257783p/archives/ee080611exp.html>, accessed 20 January 2017.



Ishank Gupta received a B.S. (2009) and an M.S. in petroleum engineering from the University of Petroleum and Energy Studies and the University of Oklahoma, respectively. Currently, he is a Ph.D. student at the University of Oklahoma. He worked as a reservoir engineer at Schlumberger from 2010 to 2015. His research interests include numerical simulation, reservoir characterization, and unconventional petrophysics.



Chandra Rai received an M.S. (1971) in geophysics from the Indian School of Mines and a Ph.D. (1977) in geology and geophysics from the University of Hawaii. He has worked as a technology director at Amoco for 18 years. Currently, he is a director and professor at the University of Oklahoma. He teaches petrophysics, petrophysics laboratory, seismic reservoir modeling, unconventional reservoirs, and well logging. His research interests include rock

physics, petrophysics, geomechanics, with an emphasis on unconventional shale gas and oil reservoirs.



Carl Sondergeld received an M.A. (1972) in geology from Queens College and a Ph.D. (1977) in geophysics from Cornell University. Currently, he is the professor and Curtis Mewbourne chair at the University of Oklahoma. He teaches petrophysics, petrophysics laboratory, technical communications, seismic reservoir modeling, unconventional reservoirs, introduction to petroleum engineering, and well logging. He coaches the SPE Petrobowl team and carries out research in the areas of rock physics, petrophysics, and geomechanics, with an emphasis on unconventional shale gas and oil reservoirs.



Deepak Devegowda received a B.S. in electrical and electronics engineering from the Indian Institute of Technology and a Ph.D. (2008) in petroleum engineering from Texas A&M University. He is currently an associate professor of petroleum engineering at the University of Oklahoma. His research interests include unconventional oil and gas reservoir engineering, high-resolution reservoir characterization, and production optimization.